EVOLUTION OF DIFFUSE NEBULAE

By William G. Mathews
University of California at San Diego
and
C. R. O'Dell
Yerkes Observatory, University of Chicago

Introduction

When one surveys the Palomar prints at low Galactic latitudes, he soon discovers the vast number of extended emission regions and the seemingly endless variety of their apparent forms. The exquisite apparent structures of many nebulae may result largely from differential extinction by interstellar particles along the line of sight and in many such cases the exciting stars are difficult to find. For other nebulae the ionized gas appears to be so symmetrically disposed about a luminous blue star (or stars) that the origin of the ionizing radiation is immediately apparent. Not all forms are chaotic and one soon notices certain characteristic shapes. Explanation of these forms and how they relate to other problems of current astrophysics is the goal of a major effort in present-day astrophysics and is the subject of this review.

It is now known (largely from radio studies) that ionized diffuse nebulae, so conspicuous on the Palomar prints, represent only about a tenth of the total interstellar gas; most of the gas is neutral, and is essentially transparent at optical frequencies. Because of the large cosmic abundance of hydrogen, the ionized and neutral clouds have become known as H II and H I regions, respectively. This fundamental dichotomy of the interstellar medium was first clearly demonstrated by Strömgren, who showed that the width of the boundary between the neutral and ionized gases is roughly equal to the mean free path of the ionizing radiation, $\lambda_i \sim (n\alpha)^{-1} \sim 0.05/n$ pc, where n is the number density of atomic hydrogen and α is its photoionization cross section. For typical values of n, λ_i is significantly less than most distance scales resolvable with large telescopes, so the H I–H II boundary is virtually a discontinuity from an astronomical point of view.

Following Strömgren's original work, theoretical studies by Spitzer (1948, 1949, 1954) and Spitzer & Savedoff (1950) showed that the temperature of the H II gas ($T_2 \simeq 10^4$°K) is generally higher than in H I regions by a factor of about 10^2. If the density on both sides of the ionization front is comparable, the difference in pressure will naturally result in an outward expansion of the ionized gas. The nature of this expansion and its general consequences was first set forth by Oort (1954), Oort & Spitzer (1955), Schatzman & Kahn (1955), and Savedoff & Greene (1955). Although these early theoretical studies were necessarily somewhat schematic, the overall picture which emerged has subsequently been verified by more detailed work.

The evolution of a typical H II region begins with a large, fairly dense H I cloud which, for reasons not entirely clear at present, is condensing into stars. As long as the stars are of spectral types later than about B5, the cloud will remain mostly neutral. During this stage there is an interplay between gravitational and gas pressure forces in the cold gas. However, as soon as a massive O (or early B) star forms and approaches the main sequence, the gas surrounding the star becomes ionized (quite rapidly if the density is low) and, owing to its substantially higher temperature, expands outward under the influence of its own internal pressure. In most cases the gravitational forces within the ionized part of the cloud can be neglected entirely. Because of the relatively low pressure in the surrounding H I gas, the H II gas expands at about its own velocity of sound, $\sim$13 km/sec for $T=10^4$°K, much as it would into a vacuum, in the first approximation. The neutral gas is, however, bulldozed ahead of the H II gas. Since the velocity of sound in the H I gas is small ($\sim$1 km/sec), the pile-up of neutral gas ahead of the expanding H II region begins with a strong shockwave behind which the neutral gas density rises (because of radiative losses) to a value which permits a rough (though not exact) pressure balance at the ionization front, despite the large difference in temperature. This configuration, consisting of a shock followed by a region of compressed H I and an ionized interior, grows in radius and moves out through the neutral cloud both spatially and masswise as the O star approaches the main sequence, emitting more and more ionizing radiation. After several million years the ionizing star will leave the main sequence, the H II region will recombine, and the expanding compressed H I shells will move out into the general interstellar medium, contributing their kinetic energies to the chaotic motions observed there.

When examined more closely this evolutionary system is seen to require modification, since the initial H I cloud almost certainly would contain interstellar particles and, to some extent at least, a magnetic field. Both of these constituents bring additional forces into play. The radiation pressure of starlight on the particles within the H II gas results in an additional source of outward momentum, which is then communicated to the gas. If the particles can withstand destruction in the hot plasma (as recent observations suggest), their presence in the ionized gas could explain the central holes observed in several H II regions. Another plausible explanation of these holes is the possibility of stellar winds. Also, magnetic forces could influence the extent of the compression in the high-density H I gas which precedes the ionization front. However, the effects of magnetic fields in this regard have not been extensively studied, nor have the observations been very helpful. Of some interest, too, is the possibility that instabilities in the compressed H I shell could result in star formation. Indeed, there are theoretical indications that gravitationally unstable condensations might be expected, and observations of ionization fronts and expanding associations have provided some limited evidence of this possibility.

Also implicit in much of the work on the evolution of H II regions has been the hope that a more complete theoretical understanding of the gas-dynamical aspects of the problem might be useful in understanding the formation of the exciting stars and the energy balance in the interstellar medium. The high density and small dimensions of several newly formed H II regions which have been studied in the 1–10 GHz region indicate that these objects have not undergone very much expansion and must be very young. The gas which is being ionized in these nebulae may provide useful information about the residual gas left behind in the process of star formation. At the other end of the evolutionary development, the rate at which the expanding H I shells supply energy to the galactic disk should be compared with the corresponding power generated by supernovae and with estimates of the energy dissipation rate by cloud-cloud collisions. We will review the present status of these areas of interest. However, we first review the basic evolutionary patterns which can occur and the various techniques which have been used to describe them.

Characteristic Lengths and Times, Gas-Dynamic Equations, Shock and Ionization Fronts

In his classical paper on H II regions, Strömgren (1939) determined the radius of the ionized sphere in a constant-density nebula produced by a hot star. A good approximation to this radius can be easily obtained by equating the ionizing photon luminosity $\mathcal{L}$ (the number of photons with energy greater than the ionization potential of hydrogen emitted by the exciting star per second) to the total rate of recombinations to excited levels of hydrogen throughout the nebula,

$$\mathcal{L} = \int_0^{R_i} n_i(R)^2\beta[T(R)]4\pi R^2 dR \qquad \text{1a.}$$

where β is the recombination coefficient. If the electron density n_i is constant,

$$\mathcal{L} = n_i^2\beta(T)(4\pi/3)R_i^3 \qquad \text{1b.}$$

so that

$$R_i = \left[\frac{3}{4\pi}\,\frac{\mathcal{L}}{n_i^2\beta(T)}\right]^{1/3} \qquad \text{1c.}$$

is the ionization radius. Recombinations directly to the ground state are ignored since they result in ionizing photons which must be absorbed at a nearby point in the nebula (on-the-spot assumption). This assumption and the neglect of helium are justified by more detailed calculations in which an equation of transfer is solved for the diffuse ionizing radiation (Hummer & Seaton 1964). The recombination coefficient to excited levels is an average of the recombination cross section over a Maxwellian electron distribution, $\beta \simeq 4.1\times 10^{-10}/T^{0.8}$ cm^3/sec. If the exciting star is approximated with a blackbody of temperature T_* and luminosity $\mathcal{L}_e$ (ergs/sec), then

$$\mathcal{L} = 2.76\times 10^{43}(\mathcal{L}_e/\mathcal{L}_\odot)f(10^{-4}T_*) \qquad \text{2.}$$

where f is a slowly varying function of order unity having a maximum at $f(7.18)=2.86$. Values of $\mathcal{L}$ obtained with Equation 2 for given values of T_* and $\mathcal{L}_t$ will tend to be somewhat larger than those based on emergent fluxes of model atmospheres of early-type stars (Rubin 1968).

Suppose a star with ionizing photon luminosity $\mathcal{L}$ is suddenly put into a very large H I cloud of rather low density n_i. Since the density is low, the radiation wave which ionizes the gas will initially move outward (supersonically), and the gas will not move appreciably. The ionization front will slow down when the cloud is ionized out to a radius R_{si} (the "initial" Strömgren sphere) given by Equation 1c. However, because of the pressure imbalance across the ionization front, gas-dynamic forces will eventually cause the H II region to expand outward until its density decreases to some value n_f where a pressure balance can be achieved across the ionization boundary, $2n_fT_2 = n_iT_1$. (Here the factor 2 appears because the particle density is doubled upon ionization and the subscripts 1 and 2 denote regions in the H I and H II regions, respectively.) In this equilibrium configuration the steady-state condition must again hold, i.e. $\mathcal{L} = n_f^2\beta(T_2)(4\pi/3)R_{sf}^3$, where R_{sf} is the radius of the "final" Strömgren sphere. Taken together with a similar equation for R_{si} and the condition for pressure equilibrium, it follows that $R_{sf} = (2T_2/T_1)^{2/3}R_{si} \simeq 34R_{si}$ and $n_{sf} = n_{si}/(2T_2/T_1 \simeq n_{si}/200$. The final Strömgren sphere also contains considerably more mass, $M_{sf} = (2T_2/T_1)\ M_{si} \simeq 200\ M_{si}$, so the ionization front must move outward masswise as the H II region expands.

The nature of the early evolution of an H II region with constant initial density n_i depends largely on the ratio $t_{\mathrm{on}}/t_{\mathrm{form}}$; where t_{on} is the time taken by the exciting star to attain its full ionizing photon luminosity as it approaches the main sequence and t_{form} is the time needed to form the initial Strömgren sphere if the same star, already on the main sequence, were suddenly placed in the nebula. If the structure of early-type protostars is approximated with a polytrope, and the stellar luminosity is assumed to be constant during the pre-main-sequence contraction (in radiative equilibrium), then t_{on}, the time required for the effective temperature to increase from 10^4 °K to T_*, its main-sequence value, can be easily derived from the virial theorem (Chandrasekhar 1939, Mathews 1965). Representative values of t_{on} and approximate effective temperatures are shown in Table I for four early-type, massive stars. The "formation time" t_{form} is actually a measure of the response time of the nebula to the stellar ionizing radiation, and is roughly equal to the recombination time scale of the gas, $t_{\mathrm{form}} \simeq (n_i\beta)^{-1} \simeq 10/n$ years. That is, if a star were suddenly placed in an H I cloud of density n_i, the rapidly moving ionization front would at first slow down because the stellar flux at the front varies as R^{-2}, but a more rapid deceleration would occur when the gas began to recombine appreciably. Values of t_{on} in Table I indicate that $t_{\mathrm{on}} \gtrsim t_{\mathrm{form}}$ as long as $n_i \gtrsim 10\ \mathrm{cm}^{-3}$, which is the case for most well-observed H II regions. To properly calculate the early evolution of H II regions, it is generally necessary, therefore, to consider in detail the rate at which $\mathcal{L}$ increases with time as the exciting star moves onto the main sequence.

TABLE I

PROPERTIES OF CENTRAL STARS AND STRÖMGREN SPHERES[a]

$M/M_\odot$	T^* (°K)	($\mathfrak{L}_s/10^5\mathfrak{L}_\odot$)	$\mathfrak{L}$ (sec^{-1})	t_{on} (10^4 yr)	t_{ms} (10^4 yr)	T_2 (°K)	R_{si} (pc)	t_{si} (10^4 yr)	R_{sf} (pc)	t_{sf} (10^6 yr)
30	42 000	1.32	8.46	2.2	4.2	7700	13.0	85	370	25.0
							0.60	3.9	17	1.1
20	35 100	0.501	2.56	2.8	6.2	7400	8.5	56	238	16.0
							0.39	2.6	11	0.75
11	27 400	0.095	0.296	5.8	12.6	7000	4.0	27	110	7.7
							0.18	1.2	4.8	0.34
6	20 200	0.0135	0.0219	15.7	35.5	6500	1.7	24	44	3.2
							0.08	0.57	2.0	0.15

[a] Note: In the last four columns, upper values for $n_i = 10$ cm^{-3}; lower values for $n_i = 10^3$ cm^{-3}.

Further insight into the general nature of the evolution can be gained by comparing t_{on} and t_{ms}, the main-sequence lifetime of the exciting star, with the times necessary for sound to cross the initial and final Strömgren spheres, $t_{si} = R_{si}/c_2$ and $t_{sf} = R_{sf}/c_2$, respectively. The isothermal velocity of sound in the ionized gas is given by $c_2 = \sqrt{2kT_2/M}$, where M is the proton mass. The temperature of the ionized gas, with approximate values listed in Table I, usually increases slightly with increasing T_*. The sound-crossing times t_{si} and t_{sf} represent the characteristic times necessary for significant gas-dynamical motions to develop in the nebula. In cases where the initial density is low and/or M_* is large, $t_{on} < t_{si}$ and $t_{ms} < t_{sf}$. The first of these inequalities indicates that the ionization front will move out in the nebula at high velocity to a distance of about R_{si} before the gas begins to move appreciably. In this case the velocity of the ionization front may move supersonically with respect to the neutral gas during its early stages (weak R fronts will develop, see below), and systematic expansion of the nebula will occur only after the initial Strömgren sphere is formed. The second inequality, $t_{ms} < t_{sf}$, indicates, however, that the central star will move off the main sequence, whereupon T_* (and therefore $\mathfrak{L}$) will decrease, causing the H II region to recombine before the final equilibrium Strömgren sphere can be formed. Conversely, for larger values of n_i and/or smaller M_*, Table I indicates that $t_{on} > t_{si}$ and $t_{ms} > t_{sf}$. The early evolution in this case is characterized by an H II region which expands away from the central star at the same time that the latter approaches the main sequence. The radius of the ionization front at any time will be given approximately by Equation 1c if the mean density and the instantaneous value of $\mathfrak{L}$ are used. [Weak D-type (dense) fronts will result, see below.] Since $t_{ms} > t_{sf}$, final equilibrium spheres are possible, at least in principle. Implicit here is the assumption that the neutral gas is not in motion when the ionization process begins. This has usually been assumed, since any supersonic motion in the neutral gas would be damped on a short time scale, and sonic motions, if they existed, would be very slow compared to c_2, which characterizes the velocities expected after ionization begins.

In spherical geometry, the gas-dynamic equations for the conservation of mass, momentum, and energy, in terms of the Lagrangian coordinate r (fixed for a particular fluid element for all time), are

$$\rho(R, t)R^2\partial R = \rho_0(r)r^2\partial r, \quad 3.$$

$$\rho(\partial u/\partial R) = -\partial P/\partial R \quad 4.$$

and

$$\partial\epsilon/\partial t = -\rho(\partial v/\partial t) + (G_{\text{II}} - L_{\text{II}})x^2 + (G_{\text{I}} - L_{\text{I}})(1 - x)^2 \quad 5.$$

respectively, where $\rho(R, t)$ is the density, $u(R, t) = \partial R/\partial t$ is the velocity, $v = 1/\rho$ is the specific volume, $P(R, t)$ is the pressure, and $\epsilon(R, t)$ represents the internal thermal energy per gram. Equation 3 states that the mass of an element of gas does not change during the evolution; initially $\rho(R, 0) = \rho_0(r)$. Equation 4 states simply that the gas is accelerated if there is a local imbalance of pressure forces. Equation 4 needs to be supplemented with an equation of state, $P = K(1+x)\rho T/M$, where $T(R, t)$ is the local temperature and $x(R, t)$ is the fraction of mass which is locally ionized. Clearly $0 \leq x \lesssim 1$. For the present we ignore additional terms

$$+ (\sigma\rho/Mc)(\mathcal{L}_e/4\pi R^2) - \rho GM(R)/R^2 - (\boldsymbol{H} \times \text{curl}\, \boldsymbol{H})/4\pi$$

which could be included on the right side of Equation 4 to account for radiation pressure on the grains (which have a mean cross section σ per proton), gravitational forces [$M(R)$ includes all mass interior to R], and magnetic forces. For simplicity, the presence of helium is usually ignored.

Equation 5 states simply that the thermal energy of a mass element decreases if it does work on the surrounding gas, and vice versa. In addition, the thermal energy per gram, $\epsilon = 3k(1+x)T/2M$, is increased or decreased by radiative absorptions (G) or emissions (L). Whenever a hydrogen atom is ionized, the thermal energy of the gas is increased by $\epsilon = \langle h\nu\rangle - \chi_0$ where $\chi_0 = 13.6$ eV and $\langle h\nu\rangle$ is the mean photon energy. Because of this process $x^2 G_{\text{II}} = (1-x)\alpha\epsilon\mathcal{L}/M4\pi R^2$, where α is the mean photoionization cross sections in the Lyman continuum and $\mathcal{L}(R, t)$ is the ionizing photon luminosity. The H I gas is heated by photoionization of those atoms and ions with binding energies less than χ_0 (Seaton 1955). Recombination radiation and collisional excitation of low-lying excited levels of various ions contribute to $L_{\text{II}}(\rho, t)$ (Burbidge, Gould & Pottasch 1963). In the neutral gas, the radiative cooling rate L_{I} results largely from radiation following excitation of H_2, oxygen, and carbon by collisions with electrons and hydrogen atoms (Spitzer & Tomasko 1968, Seaton 1958, Takayanagi & Nishimura 1960, Dalgarno & Rudge 1964, Smith 1966). The degree of ionization is increased by photoionization and decreased by recombinations, i.e.

$$\frac{\partial x}{\partial t} = \alpha \frac{\mathfrak{L}}{4\pi R^2}(1 - x) - \frac{\rho x^2}{M}\beta \qquad 6.$$

Finally, the equation of transfer for the ionizing stellar radiation is

$$\frac{\partial \mathfrak{L}}{\partial R} = -\alpha\mathfrak{L}\frac{\rho}{M}(1 - x) \qquad 7.$$

If dust is present in the ionized gas, an additional term, $-\rho\sigma\mathfrak{L}/M$, should be entered into the right-hand side of Equation 7. Given any initial configuration, Equations 3–7 and the equation of state will determine the radial dependence of the six variables ρ, u, P, T, x, and $\mathfrak{L}$ at any later time. In addition, spherical symmetry requires that $u(0, t) = 0$, and, if the central star is evolving simultaneously with the nebula, then $\mathfrak{L}(0, t)$ must also be specified.

While the complete set of equations above is difficult to solve, it is often possible to make drastic simplifications. As a rule, the internal thermal energy and gas temperature (in H II and often in H I) are determined more by the net flow of radiative energy into each element of the gas than by the work done by compression forces, i.e. $G_\pi \simeq L_\pi$. Similarly, in Equation 6, $\partial x/\partial t$ is very small outside of the ionization front, so that $x \simeq 1$ in the ionized gas and $x \simeq 0$ in the H I gas. Together with the algebraic terms in Equation 5, this condition leads to the often-used assumption that both the H II and H I gases are isothermal. Of course, real nebulae deviate to some extent from isothermality (Hjellming 1966, Rubin 1968a), but not greatly.

One curious property of the nonlinear equations of gas dynamics is that the solutions may involve mathematical discontinuities (shockwaves) in the velocity, density, and temperature, even if no discontinuities are present initially. The real width of these "discontinuities" is of the order of a collision mean free path $\lambda_s \sim (n\sigma_a)^{-1}$, where $\sigma_a \sim 10^{-16} - 10^{-15}$ cm^2 is a typical atomic collisional cross section. This is much less than typical widths of ionization fronts, i.e. $\lambda_s \ll \lambda_i$. Shocks may therefore be regarded as discontinuities with respect to the structure of an ionization front, while the latter may itself be regarded as a discontinuity with respect to the overall flow, of dimension R_{si}. This hierarchy of length scales has been described by Axford (1961) and Newman & Axford (1968).

If both shock and ionization fronts are considered as steady-state discontinuities, the equations for conservation of mass and momentum across the fronts, namely

$$\rho_1 w_1 = \rho_2 w_2 = \dot{m} \qquad 8.$$

and

$$P_1 + \rho_1 w_1^2 = P_2 + \rho_2 w_2^2 \qquad 9.$$

are sufficient to determine various "jump conditions" for ρ, u, and P. Here w is the normal gas velocity with respect to the discontinuity, $\dot{m}$ is the mass flux, and subscripts 1 and 2 refer to gas before and after traversing the dis-

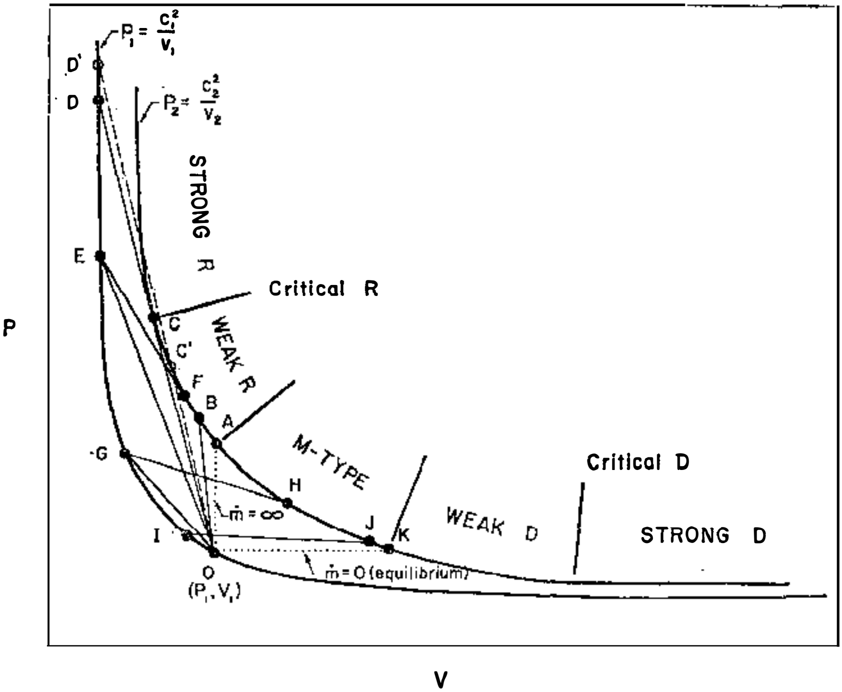

FIG. 1. Isotherms for the neutral and ionized gases, the latter marked off for various ionization fronts defined with respect to (P_1, v_1) at O. Various ionization and shock fronts are also shown.

continuity. If the velocities are eliminated from these equations, it follows that $P_2 - P_1 = -\dot{m}^2(v_2 - v_1)$, where $v = 1/\rho$. In a (P, v) diagram the discontinuous change in P and v across a front (ionization or shock) must be represented by a straight line of negative slope, with more negative slopes corresponding to discontinuities which are moving faster. Since the entropy must increase across a shock, it is easy to show that only compressive shocks (for which $v_2 < v_1$) can occur (Landau & Lifshitz 1958), although both $v_2 > v_1$ and $v_2 < v_1$ are possible across ionization fronts. Together with an analogous energy-conservation equation, Equations 8 and 9 become the Rankine-Hugoniot relations which, in effect, relate the ratio of the flow variables across the adiabatic discontinuity to the speed of the shock. For strong adiabatic shocks in a monotonic gas, $\rho_2/\rho_1 \simeq 4$ and $T_2/T_1 \simeq 3w_1^2 M/16\, kT_1$. However, if both H I and H II gases are assumed to be isothermal, then each has an equation of state of the form $P = c^2/v$, where c is the isothermal speed of sound. In Figure 1 the equations of state for both H I and H II are shown as hyperbolas, slightly distorted for diagramatic purposes.[1] Since $c \sim T^{1/2}$, $c_2 > c_1$ and the isotherm for the H II gas is farther from the origin. Isothermal shock transitions (where $c_1 = c_2$) are represented in this diagram by chords of negative slope connecting two points on the same isotherm. The compression in an isothermal shock can be quite large, since $\rho_2/\rho_1 = (w_1/c_1)^2$. Ionization fronts are represented by straight lines of negative slope between the two isotherms.

Ionization fronts have been classified by Kahn (1954) into two distinct categories; R-type (rare), for which the neutral gas has a lower density $\rho_1 < \rho_2$ (or $v_1 > v_2$), and D-type (dense), for which $\rho_1 > \rho_2$ (and $v_1 < v_2$); see also Spitzer (1968) and Axford (1961). R-type fronts move supersonically with respect to the neutral gas, and the converse is true for D-type fronts. Finally, "weak" and "strong" R-type fronts move supersonically and subsonically relative to the ionized gas respectively, and the contrary holds true for weak and strong D-type fronts. In Figure 1 the H II isotherm is marked off according to these various types of fronts defined with respect to point O on the H I isotherm. Note that $w_2 = c_2$ for both R-critical and D-critical fronts where the H I–H II transition line is tangential to the H II isotherm. The so-called M-type fronts are forbidden from point O since the slope of the discontinuity would be positive. The velocity of a rapidly moving ionization front is limited only by the flux of stellar (ionizing) photons incident at the rear of the front. In this case the mass flux is $\dot{m} = M\mathfrak{L}(R_i)/4\pi R_i^2$, where R_i is the instantaneous radius of the H II region. For slower-moving ionization fronts, however, the total recombination rate within the H II region is very large compared to the rate at which neutral atoms cross the ionization front (Axford 1964, Newman & Axford 1968). In this case, Equation 1a is very nearly satisfied at all times, even when the ionization front continues to move out masswise.

The entire history of an H II region can be schematically understood from Figure 1. Imagine, for example, a very large, low-density H I cloud having $P = P_1$ and $v = v_1$. If a massive hot star is introduced into this cloud, $\dot{m}$ is initially very large and the ionization front corresponds to the weak R transition OB in Figure 1. As the front moves out $\dot{m}$ decreases, since the flux from behind is reduced both by spatial dilution and by recombinations within the H II gas. Eventually the front becomes critical-R (OC), which also is equivalent to an isothermal shock in the neutral gas (OD) followed by a D-critical ionization front (DC) from point D. At this time the front begins to move subsonically relative to the ionized gas. Sound waves which then overtake the front from the rear combine into a shock; the shock moves ahead of the ionization front since the latter continues to slow down. Configurations such as a shock (OE) followed by a D-type ionization front (EF)

[1] In the case of shocks, subscripts 1 and 2 refer to the same gas, but for ionization fronts and in Figure 1 they refer to the H I and H II gases.

then develop, assuming the density remains constant in the shocked H I gas. The shock slows finally from OG to OI, where it is nearly sonic (i.e. it has nearly the same slope as the H I isotherm) and has expanded to infinity. Meanwhile, the ionization front also slows down as the successive transitions EF, GH, and IJ approach the limit OK (where $\dot{m}=0$ and $P_1=P_2$), which corresponds to the final Strömgren sphere, an equilibrium configuration. This describes only one idealized evolutionary scheme; if the initial H I cloud were denser, then the point (P_1, v_1) would appear higher on the H I isotherm, the front would initially be D-type, and R-type fronts might not occur at all.

Axford (1961) has made a much more detailed study of the types of steady-state, plane-parallel ionization fronts which can occur, properly allowing for the fact that the shock "discontinuity" can appear within the ionization-front structure. He has shown that the presence of radiative cooling and recombination within the ionization front permits the existence of strong D fronts. It appears then that the critical R condition, discussed above in connection with Figure 1, is not always reached. As the weak R front OF slows down, it develops an internal shock which moves forward within the front. This shock (OD′) eventually moves ahead of the front, which then develops into a strong D configuration (D′C′). Axford had also shown that ionization-front structures can exist with 0, 1, or 2 internal shocks. Such complexities, not evident from Figure 1 alone, have also been discussed by Newman & Axford (1968). A variety of weak R and weak D quasisteady, plane-parallel fronts has been worked out by Hjellming (1966), who considers radiative heating and cooling in detail, recombinations, the presence of helium, and the detailed flux spectrum at each position in the front. He has also used the emergent flux from model stellar atmospheres rather than assume blackbody radiation. The structures of these fronts show the striking effects of the hardening of stellar radiation, which can result in rather high-temperature peaks ($T\simeq 20\,000$ °K), especially in the weak R fronts. The possibility of shocks within these fronts was not explored.

The assumption of plane-parallel, quasisteady ionization fronts is valid only if $\lambda_i \ll R_i$, and if the time necessary for an element of gas to pass through the ionization front moving at velocity U_i, $t_{cr}=\lambda_i/U_i$, is much less than the time scale t_Δ during which the structure of the front changes significantly. For example, if the ionizing photon flux F from the rear is changing rapidly, then $t_\Delta \sim (d\ln F/dt)^{-1}$, or, if the neutral gas has a density gradient, $t_\Delta \sim (Ud\ln n/dr)^{-1}$. Vandervoort (1965a, 1965b) has studied the structure of plane-parallel, slightly nonsteady ionization fronts which, however, do not include recombinations or cooling. While the ionizing flux at the rear of Axford's structures must be greater than the mass flux through the front (since recombinations occur within the front itself), in Vandervoort's solutions the ionizing flux in the H II region far behind the front approaches a value F_0 which is proportional to the mass flux. Vandervoort solves for the nonsteady structure of the front for the case where F_0 is slightly time-dependent. Vandervoort (1965b) argues that the restriction that quasisteady ionization fronts cannot move directly into the neutral gas when conditions become *M*-type necessarily means that the fronts become nonsteady. This argument may not be entirely correct in every case. Although, strictly speaking, no truly steady ionization front can occur in nature, it is possible to approach this condition very closely whenever $t_{cr} \ll t_{\Delta}$. Moreover, as a weak *R* front gradually slows down, Axford's steady solutions indicate that an internal shock appears in the structure. This shock moves toward the front of the structure as U_i decreases until finally it is released smoothly into the general flow as conditions become *M*-type with a *D*-type front and a leading shock.

Because internal shocks are not considered by Vandervoort, all the flow variables necessarily vary monotonically across the front, and it is difficult to understand how a smooth transition from *R* to *D*-type (or vice versa) could occur, since a shock would have to be produced. In fact, a shock can be fitted within quasisteady *R*-type fronts, even when recombinations and cooling are neglected. Also, this shock becomes stronger when it is placed nearer to the un-ionized gas, so it appears that smooth transitions from *R* to *D*-type quasisteady fronts can occur in this case too.

Theoretical Evolutionary Models

In this section we will be concerned primarily with various attempts to solve the equations in the previous section for the evolutionary development of an H II region produced by a hot star in a large cloud of initially neutral gas. Magnetic fields and radiation-pressure phemonena will be ignored for the most part, and spherical symmetry will usually be assumed. We omit therefore a detailed discussion of the "rocket effect," the acceleration of clouds resulting from the momentum delivered by the ionized gas as it expands into a vacuum (or low-density gas) in the direction of a hot star (Oort 1954, Oort & Spitzer 1955, Kahn 1954). In all of the models discussed here, the velocity in the neutral cloud is assumed to be negligible at the start, i.e. $u(R, 0) = 0$.

The first quantitative understanding of the spherical problem emerged during the 1953 IAU Symposium on Gas Dynamics of Cosmic Clouds when Schatzman & Kahn (1955) described the ionization of a neutral cloud with constant initial density. They noted that an H II region will incorporate more mass as the density of ionized gas decreases with expansion, provided that Equation 1b holds at all times. They also showed that a shock is formed in the neutral gas, and if the density and velocity in the shocked H I gas are assumed constant, the flow is largely determined by the jump conditions at both fronts. The usefulness of this approximation, used already in connection with Figure 1, has since been pointed out by many authors. Schatzman & Kahn, however, assumed that the shock was adiabatic (instead of more nearly isothermal) and therefore underestimated the compression in the shocked neutral gas. Subsequent and more elaborate theoretical attempts on this problem have usually adopted one of three quite disparate techniques: similarity solutions, the method of characteristics, or numerical integration. Fortunately, results from these three approaches are complementary and, taken together, provide a rather complete picture of the various evolutionary patterns which can emerge. Results of each of these methods will now be discussed separately.

Similarity solutions.—In Eulerian formulation, Equations 3 and 4 become

$$\frac{\partial \rho}{\partial t} + u \frac{\partial \rho}{\partial R} + \rho \left(\frac{\partial u}{\partial R} + \frac{2u}{R} \right) = 0 \qquad 10.$$

and

$$\rho \left(\frac{\partial u}{\partial t} + u \frac{\partial u}{\partial R} \right) = - \frac{\partial P}{\partial R} \qquad 11.$$

respectively. For the case of an isothermal gas $P = \rho c^2$, and these equations are sufficient to determine $\rho(R, t)$ and $u(R, t)$ for any given initial conditions. Equations 10 and 11 can be simplified to a set of *ordinary* differential equations with a dimensionless independent variable $\eta \equiv R/ct$, provided the circumstances of the flow involve only characteristic velocities and not lengths (Sedov 1959, Taylor 1946).

Savedoff & Greene (1955) first applied this idea to H II regions by assuming that, in the first approximation, an expanding H II region could be represented by a uniformly expanding rigid sphere. With this internal boundary condition, the solutions for the flow variables in the (isothermal) H I region represent exact solutions of Equations 10 and 11 for all R and t. Savedoff & Greene showed that a shock (which must have a uniform expansion velocity) is necessary to connect the solution between the spherical piston and the undisturbed gas, which is assumed to have $\rho(R, 0) =$ constant and $u(R, 0) = 0$ initially. According to their model, the shell of H I gas between the fronts is compressed by a factor of 200 owing to the isothermal shock. The width of this shell increases quite slowly during the evolution; the shock therefore moves only slightly faster than the ionization D-type front, which expands out at $U_i \simeq c_2 \simeq 14$ km/sec. Kaplan (1959, 1966) has also discussed several simplified similarity solutions for plane-parallel ionization fronts and H I regions which behave either adiabatically or isothermally. His results are qualitatively similar to the more detailed treatments of the spherical problem which we now describe.

Goldsworthy (1958, 1961) has developed a similarity solution which also gives $u(\eta)$ and $\rho(\eta)$ within the ionized gas and allows the ionization front to expand masswise in a natural way. He showed, however, that spherically symmetric similarity solutions, in which the ionizing photon luminosity of the central star is assumed to be constant, necessarily require that the gas temperature vanish at the origin, which is physically unacceptable. For this reason Goldsworthy solved the problem in cylindrical symmetry in terms of $\eta = R/ct$, where R is now the distance from the central axis. A similarity solution is then possible if the "cylindrical ionizing star" has constant photon luminosity per unit length, the H II region is isothermal and completely ionized ($\partial x/\partial t = 0$, $x \simeq 1$), the H I gas behaves adiabatically, and the initial density varies as $\rho(R, 0) = \omega_0/R$, where ω_0 is a constant. Furthermore the ionization front is represented as a discontinuity, and the jump conditions, given by the quasisteady ionization fronts calculated by Axford (1961), were used to join the similarity solutions in the neutral and ionized regions.

One interesting feature connected with the Axford-Goldsworthy synthesis is that the similarity solutions alone (for a given ω_0) may give an infinity of possible flow patterns involving shocks and ionization fronts, yet a corresponding overdeterminacy in the ionization-front structure exactly offsets this indeterminacy. The uniqueness of the similarity flow follows from the constraint that the "discontinuities" introduced into it must correspond to physically valid structures. Goldsworthy found that the nature of the cylindrical similarity flow depends largely on the parameter ω_0 in the initial density distribution. For $\omega_0 = \omega_{0c}$ the ionization front combines with the shock in an unusual strong R configuration; but, for $\omega_0 < \omega_{0c}$ the only possible solutions are those which allow isothermal shocks within the ionized regions, the latter bounded by weak R ionization fronts. Presumably the isothermal shock is simply a result of the steep initial density gradient, and would also appear if the gas were instantaneously ionized (Pack 1953, Kahn & Dyson 1965).

Recently, Newman & Axford (1968) have solved the complete similarity flow in spherical geometry for a nebula with constant initial density ρ_0. In this case, however, a similarity solution is possible only if the ionizing photon luminosity of the exciting star $\mathfrak{L}(0, t) = S_*(t/t_*)^3$, where S_* and t_* are constants. It is a happy coincidence that the ionizing radiation of real stars does turn on at approximately this rate, as can be seen from more detailed stellar models (Mathews 1965).

Newman & Axford assume that Equation 1a holds throughout the evolution and that, as far as the overall flow is concerned, the ionizing photon flux on the back of the ionization front is negligibly small. This is valid for all except the most rapidly moving weak R fronts. Newman & Axford consider both isothermal and adiabatic conditions in the H I gas. Their solutions for the similarity flow pattern were made unique with exactly the same method used by Axford and Goldsworthy. The allowed similarity solutions obtained by Newman & Axford can be characterized with a single dimensionless constant $\Gamma = 4\pi\beta\rho_0^2 c_2 t_*^3/S_* M^2$. An entire sequence of solutions for different values of Γ shows that the velocity of the ionization front decreases monotonically with increasing Γ. For example, if the neutral gas behaves isothermally, solutions involving weak R, critical D, and weak D fronts are possible for various ranges of Γ as Γ increases. Although each of these solutions (with constant Γ) corresponds to a flow which maintains a given type of ionization front for all time, it is possible to imagine that in a real nebula the solutions would change from one kind of front to another as if Γ were changing slowly with time.

It should also be mentioned that Goldsworthy (1967) has discussed the evolution of H II regions in which gravitational forces are important. However, in describing most observed H II regions the gravitational term in the equation of motion can be neglected, at least in the ionized gas.

Method of characteristics.—In a series of papers, Vandervoort (1963a, 1963b, 1964) has discussed the initial flow which develops in the ionized gas when a hot star is abruptly "turned on" in an infinite, homogeneous cloud of neutral gas. Specifically, he has solved for the nonsteady (nonsimilar) isothermal flow behind a supersonically expanding weak R front up to the point at which the ionization radius reaches R_{si}. Since $\rho(R, 0) = \rho_0$ and $u(R, 0) = 0$, the gas only begins to move after it is overtaken by the ionization front, which is treated as a discontinuity. Additional boundary conditions are provided by the velocity and density just behind the weak R front (given by Equations 8 and 9). In the first two papers (1963a, 1963b) Vandervoort assumes that no recombinations occur within the ionized gas, but in the third (1964) the effects of recombinations are included.

In his first paper (1963a), Vandervoort solves the linearized versions of Equations 10 and 11 for part of the (R, t) plane; for the remainder he develops an approximate solution in terms of an expansion which makes use of the fact that $t_{\text{form}} \ll t_{si}$ for weak R fronts (see Table I). In later papers the method of characteristics is used (Courant & Friedrichs 1948, Landau & Lifshitz 1958, Gershberg 1961, Kahn 1954). Using this method, Vandervoort solves for the unknown functions $u(R, t)$ and $\rho(R, t)$ by numerical iteration, again making use of an expansion based on the fact that $t_{\text{form}} \ll t_{si}$. In the solution that results, the gas velocity increases monotonically with R up to the front, where its value approaches c_2 as $R \rightarrow R_{si}$; the density is fairly constant with R but reaches a maximum at the front. Apparently Vandervoort's solution differs from the similarity weak R flow of Newman & Axford largely because of the different assumptions concerning $\mathcal{L}(0, t)$. We note that Vandervoort assumes $t_{\text{on}} \ll t_{\text{form}}$, a situation which is not expected to occur very often (Table I). He has also made a model for the Orion Nebula, a rather high-density H II region, using the same approximation (1964a). None of his solutions involves shock fronts in the H II region (or elsewhere).

Calculating the extremely early stages of evolution of H II regions, Vandervoort (1966) has estimated the rate of turn-on of the ionizing photon luminosity $\mathcal{L}(0, t)$ using approximate evolutionary tracks of protostars. The flow in the ionized gas with constant initial density is solved (for weak R conditions) to the time that the ionization radius is comparable to the thickness of the front itself. At the end of the calculation only $10^{-7} M_\odot$ of gas is ionized out to a radius of $\sim 10^{-4}$ pc (for $M_* = 30\ M_\odot$), and the exciting star has a temperature of only 5000° K. It would seem, however, that the gas flow at these early times (10^2–10^3 years) could have no significant, long-lasting effect on the flow patterns during more relevant time scales (10^4–10^5 years). In any case, the gravitational term in the equation of motion, which has been neglected, would be dominant during these extremely early gas flows.

Numerical methods.—Less romantic, perhaps, but more powerful is the use of large computers for solving initial-value problems by purely numerical methods. For this purpose, the dependent variables are replaced by a set of discrete unknowns on a double mesh in the (r, t) plane. The basic pattern of differencing the differential equations is generally straightforward and is described by Richtmyer & Morton (1967). The differenced form of Equations 3, 4, and 5 together with $u = \partial R/\partial t$ and an equation of state permit an explicit and sequential solution for the dependent variables after each new time-step is chosen.

The first attempt at a numerical solution for a dynamical model of an H II region was made by Mathews (1965). The structure of the (nonsteady) ionization front was calculated as an integral part of the overall flow. For this purpose it was necessary to solve differenced forms of Equations 6 and 7 as well as the gas-dynamic difference equations discussed above. Mathews also included the effects of the hardening of the radiation at the outer parts of the nebula due to the ν^{-3} dependence of α_ν. The mean value $\alpha = \langle \alpha_\nu \rangle$ (in Equations 5, 6, and 7) decreases with radius and $\langle h\nu \rangle$ increases. The particular model calculated by Mathews (1965) included the gradual turning-on of the Lyman continuum based on an unpublished pre-main-sequence model for a 30 $M_\odot$ star computed by Bodenheimer. The combined time-dependencies of the stellar effective temperature and luminosity for this star result in $\mathcal{L}(0, t) \sim t^3$, which holds approximately until the star reaches the main sequence, at which time $T_* = 42\,000$, $\mathcal{L}_e = 1.3 \times 10^5\, \mathcal{L}_\odot$, and $\mathcal{L} = 8 \times 10^{48}$ sec^{-1}. This star is assumed to form in a quiescent cloud of constant initial density $n = 10$ cm^{-3}. As Table I indicates, the calculations show that a weak R ionization front moves directly into the neutral gas, initially at high velocities ($U_i > 800$ km/sec). However, as $R_i \rightarrow R_{si}$ the front becomes sonic with respect to the ionized gas, a shock forms and a D-type front develops. At this point the calculation was terminated. The general development of the front agrees qualitatively with the steady fronts of Axford (1961). The star reaches the main sequence just before the initial Strömgren sphere is reached. As the ionization front moves outward, its structure widens (by a factor of 30) because of a decrease in α, which is due to a hardening of the radiation and an increase in T_*. Since $\langle h\nu \rangle$ increases, the gas is strongly heated in the front as in those calculated by Hjellming (1966), and a quasisteady positive temperature gradient develops within the bulk of the ionized gas. This gradient damps out the velocity field predicted by the purely isothermal models (Vandervoort 1963a, 1963b, 1964b).

A much more complete numerical investigation into the evolution of H II regions has been made by Lasker (1966), who carried the solution far beyond the weak R stage. He regarded the ionization front as a discontinuity with respect to the flow (artificially broadening it in a manner analogous to the use of artificial viscosity for shocks) and was then able to use a simple isothermal equation of state for the ionized gas. While the details of the ionization-front structure are not given by the calculations, the simplicity of the resulting difference equations made it possible to compute many models having various initial density configurations. Lasker uses a simplified expression for the radiative heating-cooling term in the neutral gas, namely $(G_I - L_I) = c_v(T - T_0)/\tau$, which involves the specific heat c_v, an equilibrium temperature $T_0 = 100°$ K and a characteristic cooling time τ. A better representation would also involve a factor of ρ, but the general nature of the solutions is not seriously affected by this alteration.

In all specific models discussed by Lasker, the exciting star is assumed to form instantaneously in a quiescent neutral cloud of indefinite size having temperature $T_0 = 100°$ K. In his first three models the initial density is taken to be constant at $\rho(R, 0)/M = \rho_0/M = 6.4$ and 64 cm^{-3}, and radiative cooling in the neutral gas is neglected ($\tau = \infty$). The results of the first of these calculations are shown in Figure 2. The first two or three of these models correspond to the initial stages studied by Vandervoort (1963a, 1963b, 1964b) and Mathews (1965). The expanding shell of compressed neutral gas, quite striking in subsequent models of this sequence, slowly increases in width as the shock moves away from the ionization front. The leading shock decreases in strength both because of the geometrical divergence and because the density and pressure in the ionized gas diminish with time. The velocity field is somewhat more complicated. Large-amplitude waves appear to be produced whenever the flow changes significantly on a time scale short compared to the sound-crossing time in the ionized gas.

It is interesting to compare Lasker's results in Figure 2 with similar calculations made at both higher and lower initial densities. For example, the relative thickness of the compressed neutral gas appears to increase for larger values of ρ_0. Moreover, the shock velocity varies approximately as $U_s \sim \rho_0^{-2/5} t^{-1/5}$, a dependence derived by Lasker from general considerations. He has also completed models for $\tau = 10^5$ and 5×10^4 years with $\rho_0/M = 6.4$ cm^{-3}. In general, the pressure in the shocked neutral gas is determined largely by the boundary conditions at the D-type ionization front. The density distribution in the ionized gas and pressure in the dense H I shell are therefore rather independent of τ, but the density in the neutral shell varies inversely with temperature in such a way that longer cooling time scales result in thicker H I shells of lower density. Other factors which could increase the widths of the compressed neutral shells might be transverse magnetic fields, cosmic-ray pressure, gas turbulence, and a decrease in the driving pressure of the H II region (and a corresponding weakening of the leading

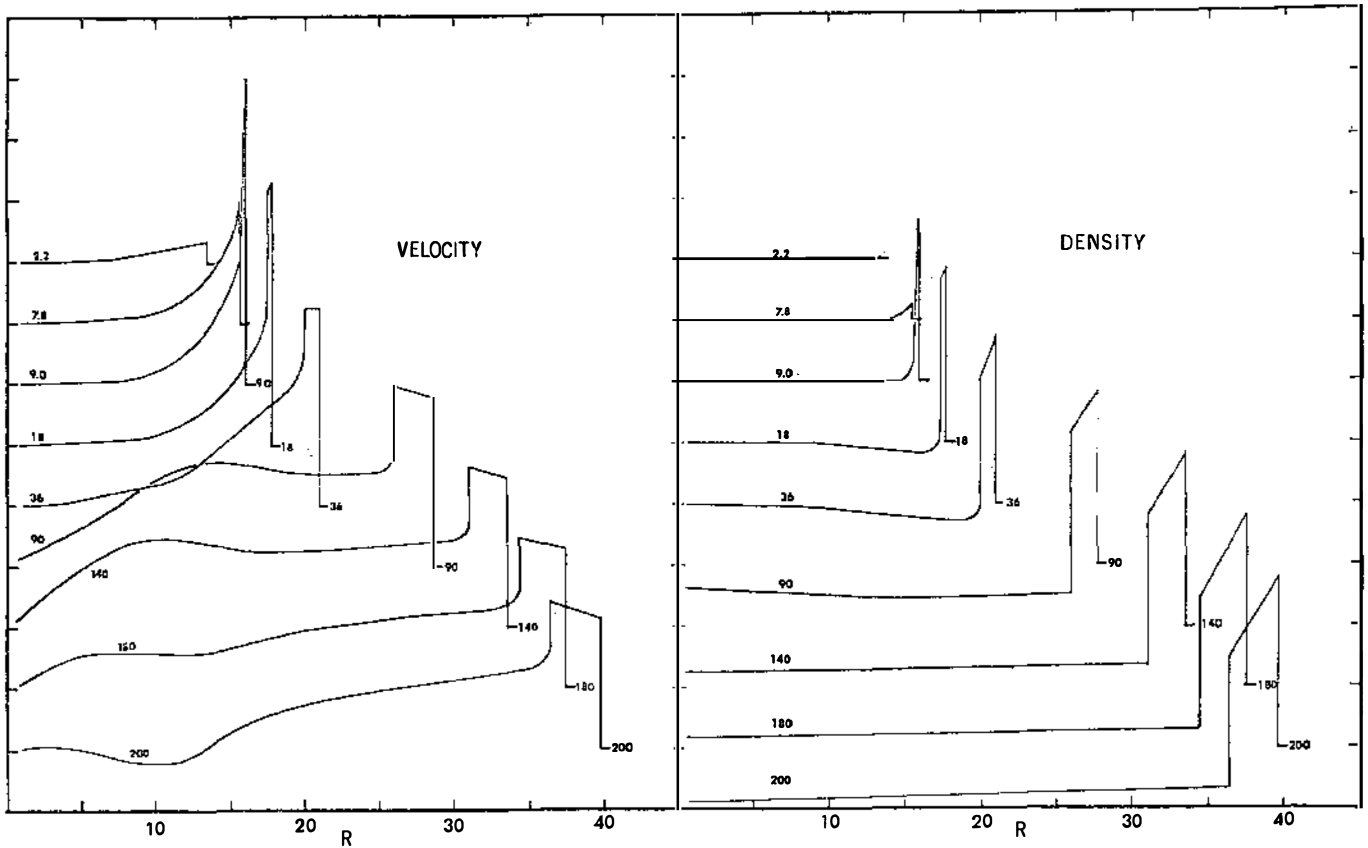

FIG. 2. Variation of gas velocity and density with nebular radius in parsecs obtained by Lasker (1966) for $\rho_0 = 6.4$ cm^{-3}, $\mathfrak{L}_* = 2.45 \times 10^{48}$ sec^{-1}. Times in 10^4 years label each curve. Vertical units are $c_2/4$ for velocity and ρ_0 for density.

shock) due to a decrease of $\mathcal{L}(0, t)$ as the central star evolves away from the main sequence. Finally, Lasker has calculated the evolution of a model with an initial density given by the isothermal function (Chandrasekhar & Wares 1949, Vandervoort 1964a) superimposed on a constant background density of 6.4 cm^{-3}. The central density $[\rho(0,0)/M = 64\ cm^{-3}]$ is not very large in this model, and by the time the ionization front moves into regions where $\rho(R, 0)/M \simeq 6.4\ cm^{-3}$ the flow pattern resembles flows computed for the constant initial-density models. No shocks appear in the ionized gas.

Davidson & Harwit (1967) have discussed the evolution of nebulae associated with massive O and B stars which form within small ($\sim$1 pc) dense ($n \sim 10^4 - 10^5\ cm^{-3}$), dusty neutral clouds. The extinction renders the bright star(s) unobservable, but much of the radiation energy is absorbed and re-emitted by the dust in the infrared. As the gas becomes ionized, a thermal radio spectrum also appears. Davidson & Harwit describe in schematic terms the expansion of these high-density nebulae under the joint influence of radiation and gas pressure. Recently Mathews (1969) has solved a similar problem in more detail. Since the initial density is high ($n \sim 3 \times 10^4\ cm^{-3}$) in his model, the ionization front is D-type until the edge of the gas cloud is reached, at which time the nebula, fully ionized, expands into the surrounding vacuum (or low-density medium). The evolution of the radio-flux spectrum is also calculated, and the results indicate that time variation at optically thin frequencies might be observable. The solution is not greatly influenced by the effects of radiation pressure on the dust. However, during the final stages of this calculation, the outer parts of the nebula are cooled by expansion faster than the radiative thermostat ($G_{\rm II}-L_{\rm II}$) can operate, which may explain certain observations of temperature gradients in diffuse and planetary nebulae.

Although more detail can be included in numerical integration of the gas-dynamic equations, compared to purely analytical methods, some of the numerical calculations may not be entirely free of error. The difference equations used in a particular calculation should be checked by attempting a numerical duplication of the similarity solutions of Goldsworthy or Newman & Axford and an overall energy check should be made.

Magnetic fields.—There is considerable evidence for a magnetic field in the general, low-density interstellar medium (Spitzer 1962) whose average intensity is of the order of 5×10^{-6} gauss. If such a field also exists in an evolving diffuse nebula, it can significantly alter the gas-dynamical picture presented above.

The general effects of a magnetic field on an evolving nebula were first roughly outlined by Abe, Sakashita & Ono (1963) and a more refined treatment was then given by Lasker (1966a, 1966b). Only very idealized cases have been considered, being those where the magnetic field is homogeneous and permeates the entire nebula, including both the ionized and un-ionized regions. The qualitative agreement of the irregularities of forms of the observed nebulae with the changes expected on introducing a magnetic field indicates that magnetic fields may play an important role in the structure and evolution of nebulae.

Lasker (1966b) has considered in detail the effects of introducing a magnetic field in the theoretical models for evolving diffuse nebulae. He shows that for the *R*-type front, i.e. where the ionization front is moving out into the gas at a highly supersonic speed, the solutions of the relevant equations differ only little from those valid for a field-free model. This is primarily because there is very little compression of gas during this phase and the relative importance of the magnetic-pressure terms remains at the assumed initially low values. The situation is considerably more complex and the role of the magnetic field is much greater for the *D*-type front, where the ionization front is moving slowly into the neutral gas and is preceded by a shock front. In this case, the increase in neutral gas density due to cooling behind the shock will be limited by the magnetic pressure, and the zone between the shock and the ionization front will be broadened. Such effects are very sensitive to the orientation of the magnetic field with respect to the fronts, with the maximum effects occurring when the fronts are moving parallel to the field, thereby causing the compression of the maximum number of field lines. This sensitivity to orientation could be expected to cause noticeable asymmetries. Because of the formidable mathematical difficulties encountered and the rather ad hoc nature of the assumptions that must be made, relatively little theoretical work in this direction has been done and many problems of basic importance in understanding the evolution of diffuse nebulae remain to be evaluated.

Stellar winds.—In the search for an explanation of density decreases in the center of the Rosette Nebula, Mathews (1966) has considered the role of mass loss from the central stars. He calculated the velocity fields and density distributions that would be expected for an evolving nebula, which, in addition to the usual effects described earlier in this article, contained shock interactions between the nebular material and a stellar wind with several assumed rates of total mass loss. It was seen that a total mass-loss rate for the entire illuminating cluster of $10^{-5}M_{\odot}$/year would produce a central density minimum similar to that which is observed. There are many uncertainties of detail in formulating this problem but the recent indications of significant mass loss from early spectral-type supergiants (Morton 1967) may indicate that this type of kinetic energy transfer could be important. Pikelner & Sheglov (1968) have also considered the effects of rapid mass loss through a stellar wind.

Role of radiation pressure.—The existence of particulate matter in the diffuse nebulae can have considerable effect upon the dynamical evolution of the region and has been the subject of several recent studies. Grains within

H II regions are expected to be positively charged because of the photoelectric ejection of electrons caused by absorption of stellar ultraviolet photons. Because of their positive charge, one expects these particles to resist collisional destruction by ions in the almost totally ionized nebulae. Subject to considerable forces by radiation pressure, the particles would be repelled from the central stars if it were not for the very efficient Coulombic drag that ties the gas and charged dust particles together (Harwit 1962). The early study by Shain, Haze & Pikelner (1954) indicated that the ratio of surface brightness of their bandpass centered on Hα and a point in the nearby continuum could be explained on the basis of an atomic continuum.

A more recent series of investigations (O'Dell & Hubbard 1965; O'Dell, Hubbard & Peimbert 1966) (made at bluer wavelengths, where one would expect the scattered light contribution to be greater and using the uncontaminated Hβ line as a standard) indicate that many diffuse nebulae have a continuum radiation in the blue that is significantly stronger than expected from atomic processes. It is very difficult to detail from which parts of the nebulae this scattered light arises, but in those few objects having symmetric outlines and studied in several parts, the surface-brightness distribution in the continuum is fit relatively well by models with a constant gas/dust ratio throughout the entire nebula, and assuming isotropic scattering. If the particles are forward scatterers, the material may be further from the bright stars.

The radiation-pressure force on an individual grain of radius a at a distance R from a cluster of illuminating stars is:

$$F_{\rm rad} = (\pi a^2/4\pi R^2 c) \sum \int_0^\infty L_s(\nu) Q_{pr}(2\pi a/\lambda) d\nu \qquad 12.$$

where $L_s(\nu)$ is the luminosity of an individual star in the cluster and the summation is made over all illuminating stars. The most luminous stars will be very blue, so that the condition $a/\lambda \gg 1$ may be satisfied, which would mean that the radiation-pressure efficiency factor Q_{rp} would approach unity. To evaluate the magnitude of this force quantitatively one needs to know the ultraviolet luminosity properties of the illuminating stars and the characteristics of the particles. Through the extensive work on model atmospheres for early-type stars (Mihalas 1964), the former is probably better understood than the latter. The observations (Krishna Swamy & O'Dell 1967) enable one to determine the effective scattering cross section per proton $\sigma' = N_p \pi a^2 Q_{\rm scat}/N_{\rm H}$ where the number density of particles N_p, the scattering efficiency ($Q_{\rm scat}$), and the effective radius (a) are weighted averages determined for the wavelength of the observations. In this case the force due to radiation pressure would become $F_{\rm rad} = (\mathcal{L}_e/4\pi R^2)\sigma' Q_{rp}/cQ_{\rm scat}$ where Q_{rp} has been appropriately weighted over the stellar flux distribution of total energy luminosity $\mathcal{L}_e$. Direct application of this formula may lead to a significant underestimate of the total force since the particles primarily contributing to the scattered light may not be the same as those important in producing the radiation-pressure effects.

The most detailed treatment of a model nebula including the effects of radiation pressure is that of Mathews (1967), where he uses density and size parameters appropriate for the Rosette Nebula,[2] and where he shows that an initially constant-density nebula develops a central hole which persists, in modified form throughout the remaining evolution of the nebula, provided the grains are not destroyed.

The principal uncertainty about the role played by radiation pressure acting on the interstellar particles is the lifetime against destruction within the ionized regions. The important source of destruction is probably sputtering, the erosion of the particles due to collisions with ions in the surrounding plasma, which eject atoms, ions, or radicals from the particle surface. Photosputtering, the dissociation of atomic fragments at the particle surface, may also be important.

Particles in the ionized region of the nebula will be subject to continuous bombardment by the ions present, primarily those of H^+, He^+, and some He^{++}, in addition to electrons. Because of their low mass and momentum, electron collisions have very little erosive effect on the particles, but colliding electrons which remain on the grain will influence the charge balance. The impact of energetic ions transfers considerable momentum to atoms in the particle, leading to ejection of atoms and ions at a rate proportional to the gas density. A simplified treatment of this phenomenon is given by Mathews (1969), based on the theory of Langberg (1958) and the experimental results of Wehner (1958). Mathews has shown that dirty ice particles will be sputtered away in time scales of less than 10^4 years if the electron density exceeds about 10^3 cm^{-3}, the exact rate being very sensitive to the particle charge.

The exact charge on an individual particle will depend upon the steady-state condition reached under the effects of photoelectric ejection of electrons and the sorption of electrons and protons, depending critically on the conditions prevailing. For example, in the early stages of evolution of an H II region the stellar temperature is low, as the star contracts to the main sequence, and the charge on the particles is less positive so that sputtering might occur more rapidly. Likewise, as an expanding ionization front passes through a region in the nebula the leading edge could cause the rapid sputtering of grains before the strong, charge-producing, stellar radiation became dominant.

[2] The grain radius of $a = 3 \times 10^{-5}$ cm used by Mathews is inconsistent with the cosmic abundance of C, N, and O. The results of his paper are still valid if a larger number of small ($a \simeq 10^{-6}$ cm) particles are assumed.

Comparison of Theoretical and Observed Nebulae

We have discussed in some detail the theoretically predicted time evolution of diffuse nebulae. Although the broad features of this evolution are fairly well understood, there remain many uncertainties, especially when one is dealing with nonhydrodynamic forces. It is, therefore, important to obtain accurate observations that will permit one to discriminate between various possible models and to understand the forces operating.

We are able to determine several nebular parameters for purpose of comparison with our models. The most straightforward is the density distribution, with determination of the velocity field being the next easiest. Although one can also determine the ionization and temperature distribution, very little has been done in this area and one is essentially limited to a discussion of the density distribution, supplemented in a few cases by knowledge of the velocity distribution. However, a significant pair of papers by Terzian, Mezger & Schraml (1968) and Mezger & Ellis (1968) show that temperatures obtained from the radio recombination lines are greater than those obtained from self-absorption turnover. The latter temperature refers to the outermost parts of the nebulae which may be expanding and cooling.

Characteristic density distributions.—One views the three-dimensional nebulae projected onto the plane of the sky, so that any interpretive investigation is actually dealing with information that is smeared by integration over the line-of-sight through the nebula. This smearing effect is minimal if the nebula possesses a high degree of three-dimensional symmetry and, fortunately, many nebulae seem to satisfy this condition.

For a given frequency and electron temperature, the brightness temperature of the radio continuum arising from free-free emissions can be related to $\int N_H N_e dl$ (the emission measure) where the subscripted variables are the hydrogen and electron densities while dl is the incremental line-of-sight through the nebula (Oster 1961). After the electron temperature has been determined, for example, from the shape of the low-frequency radio cutoff due to self-absorption (Terzian, Mezger & Schraml 1968) or from the ratio of radio recombination lines compared to the nearby continuum (Mezger & Palmer 1968), one can then derive the density distribution as a function of position (Terzian 1965, Mezger & Henderson 1967). This same basic technique can be used to interpret isophotes of recombination lines made in the optical window (Dickel 1968). The principal difficulty at the latter wavelengths is the necessity for corrections for interstellar extinction, which can vary across the face of the nebula.

Observations of the 21-cm emission line of neutral hydrogen provides a valuable supplementary study to investigations of the ionized component (Riegel 1967, Raimond 1966, Wade 1958). Direct measurements of the neutral outer envelope can determine the density distribution and total mass of the un-ionized component of the diffuse nebula. Relatively few such observations have been made, largely because of the difficulty of identifying the

TABLE II

PROPERTIES OF SOME NEBULAE WITH OBSERVED H I SHELLS

Nebula	Inner radius r_i(pc)	Outer radius r_s(pc)	$1-r_i/r_s$	Reference
Rosette	20	50	0.60	Raimond 1966
NGC 6910	1.5	5.5	.73	Davies & Tovmassian 1963
λ′ Ori	13	30	.57	Wade 1958
II Mon	40	90	0.66	Girnstein & Rohlf 1964
IC 5146	1.5	3.3	0.45	Riegel 1967
NGC 281	7.5	15	0.5	Riegel 1967

H I features arising from the particular nebulae under consideration among the many H I clouds found in the same line-of-sight along the Galactic plane. In Table II we give the results of several radio investigations as summarized in part by Lasker (1966a). The H I shells are generally rather broad and certainly exceed the ratio of inner to outer radii indicated by the evolutionary models in Figure 2. As we have seen, the theoretically expected H I shells would be broader and density concentrations less if a magnetic field was present.

Distributions of the particulate matter are even more difficult to determine, although the optical appearance of a ring of avoidance of stars around a bright H II region certainly indicates the presence of obscuring material. Direct observations of scattered light within the ionized regions are possible, but difficult, because of the contamination by the continuum of atomic origin (O'Dell et al. 1966).

Inspection of various density profiles indicates that three broad classes of density distributions can be seen: centrally condensed; quasihomogeneous; low-density centers. The first class can be identified with relatively young nebulae, although H II regions without central concentrations are not necessarily old. The quasihomogeneous nebulae are difficult to relate to a particular evolutionary state or initial condition. The nebulae having central density minima are probably those objects in which radiation pressure or stellar-wind effects are important.

Velocity fields.—Use of the observed velocity fields to discriminate between various states and conditions of nebular evolution in actual diffuse nebulae presents formidable difficulties. The range of velocities expected may be relatively small, particularly if the nebula is bounded with a *D*-type front and observations of velocity fields are confused by the effects of line-of-sight integration through the nebula. The actual expected changes in velocity often occur over relatively small distances as seen in Figure 2 and these specific locations are hard to isolate in the integrated views of the nebula. Attempts to observe velocity fields are vital and should be encouraged.

The ionized component can be studied by measurement of the radial velocity of both the radio and optical recombination lines and the optical, collisionally excited forbidden lines of ions such as O^+ and N^+. The neutral hydrogen component can be studied with rather good velocity resolution although rather poor spatial resolution, in contrast to the optical lines, but the problem of identification is very difficult, since there usually are many H I clouds along the line-of-sight.

Riegel (1967) has found that in the two nebulae in which he could find clear evidence for the association of H II and H I (NGC 281 and IC 5146) the radial velocities of both the ionized and un-ionized gas were essentially identical with no large-scale expansions greater than a very few km/sec.

The principal problem in determination of velocities from the optical emission lines lies in the extremely low surface brightness of most nebulae. High dispersions are required to study internal velocities. With ordinary spectrographs this means long cameras and relatively slow focal ratios. Although considerable data determined by slit spectrographs on the mean velocities of H II regions now exist (Miller 1968), slit-spectrograph data suitable for the study of the velocity field within a given nebula only exist for the brightest objects (Wilson, Munch, Flather & Coffeen 1959).

The use of a photographic Fabry-Perot etalon (Vaughn 1967) for the study of velocities offers significant gains in speed of observation and this method has been developed and used extensively by Courtes (1960) and his collaborators (Courtes, Georgelin, Monnet, Pourcelot 1968). The accuracy of these results for individual points is usually about 4 km/sec, which approaches incisive usefulness when one considers the moderate spatial resolution employed. Pottasch (1965) concludes from the widths of Courtes' Hα lines that velocities of expansion greater than 5 km/sec do not exist. Rather surprising, and perhaps less accurate, results have been obtained by Gershberg & Sheglov (1963) who found internal velocities of ± 50 km/sec in NGC 6618, ± 25 km/sec in NGC 6523, and ± 10 km/sec in NGC 7000 [newer results on NGC 6618 and 1976 are given in Sheglov (1968) and Pikelner & Sheglov (1968)] while Vaughn (1968) has used his photoelectric Fabry-Perot instrument to determine velocities and line profiles in the Orion Nebula.

Gaseous structures in the Orion complex.—The presence of a complex of young stars in the constellation Orion, closely mixed with known amounts of interstellar material, and its relatively high Galactic latitude make this a particularly interesting region for studying the effects of evolution of diffuse nebulae. It contains both a region of high surface brightness and small scale (the Great Nebula in Orion, M42) and a large nebula of rather low surface brightness (the Barnard Loop).

The Great Nebula in Orion has been the subject of numerous discussions and investigations. The emission-line ratios have been determined with some degree of accuracy (Liller & Aller 1959; Kaler, Aller & Bowen 1965) and the velocities and velocity profiles have been determined both for optical emission lines for forbidden and permitted features (Wilson et al. 1959, Kaler 1967) and in the radio recombination lines of hydrogen (Hoglund & Mezger 1965). It was found that a general trend exists toward lower states of ionization at increasing distance from the illuminating group of stars, the Trapezium. It was also shown that the intrinsic linewidth corresponds to a velocity of 17.5 km/sec of which 12.8 km/sec could be attributed to a thermal broadening at a temperature of 10 000° K (Weedman 1966). The extra line broadening is due to mass motions on a small scale in the nebula and the recent indications of electron temperatures lower than 10^{4}° K (Goldberg 1966) would indicate an even larger internal mass motion.

Kaler (1967) has shown that a systematic velocity difference exists in the Great Nebula, depending on the state of ionization. Ions having low ionization potentials have small negative radial velocities with respect to the Trapezium while there is a smooth change of velocity with ionization potential up through Ne^{++} at 41 eV which has a velocity of -14 km/sec. The agreement of the low angular resolution radio recombination line profiles with artificially broadened line profiles using the small-volume mass motions and temperatures (Weedman 1966) indicates that there are no systematic motions in the nebula that are obscured optically.

The density distribution has been studied both by radio observations of the thermal continuum (Menon 1961), and by the method of forbidden-line ratios (Osterbrock & Flather 1959). The results of both methods are closely tied to the symmetry of the model used (both studies assuming spherical symmetry about the Trapezium). Central densities of about 10^4 electrons/cm^3 are found from the forbidden lines while central densities of about 10^3 electrons/cm^3 are found from the radio observations. This difference is probably due to the assumed existence of rather high-density regions, which are averaged out in the broad radio-antenna beam width (Peimbert 1967). The radio-determined density diminishes smoothly from the central value to about 10^2 electrons/cm^3 at a displacement of 1 pc and 10 electrons/cm^3 at 3 pc. It is evident from the previous theoretical discussions that a strong concentration of material to the center cannot exist for long periods of time.

Vandervoort (1964a) has made the most complete analysis of M42, based upon his own calculations of the establishment of the ionization structure in the nebula. He assumes that the initial density distribution was isothermal, and by comparison of the theoretical density distribution and velocity expected at various times for his model nebulae he concluded that the age of the nebula was only about 18 000 years. Although there is considerable uncertainty in this result [Vandervoort points out the sensitivity to the assumed initial density and velocity distributions and his assumption that the ionizing flux from the illuminating stars "turned on" abruptly (the shortcomings of this assumption are obvious from Table I)], it seems doubtful if this gas-dynamical age is greatly in error. As Vandervoort points out, this small ionization age would indicate that the Trapezium stars have only recently formed while the existence of lower-mass stars on the main sequence indicates that some star formation has been occurring for much longer periods. In the absence of a good understanding of the processes of star formation, one might accept this dynamical age as evidence for the very recent origin of these illuminating stars. If, however, the nebula is not symmetric with respect to the early-type stars, then the true density distribution can be very different from that used in these calculations and the ionization age becomes an open question.

The straightforward assumption of spherical symmetry has been challenged by Würm (Würm & Perinotto 1965) who argues that the nebula is incompletely observed optically as a result of the extinction produced by large amounts of particulate matter inside the nebula. Würm derives models for M42 where the Trapezium lies to the front of the emitting gas. Certainly large amounts of dust are present in the nebula, as evidenced by the optical appearance of several dark lanes and the presence of strong scattered light (O'Dell & Hubbard 1965); but it is very difficult to evaluate Würm's model quantitatively. Although we have described here the results obtained under the assumption of spherical symmetry, the limitations of this model should be kept in mind.

The Barnard Loop (Barnard 1895) is a part of the large complex of material enveloping almost all of the early-type stars in Orion. The brightest portions in the optical region are in the north-east quadrant and have an emission-line spectrum. A much more amorphous and continuous structure

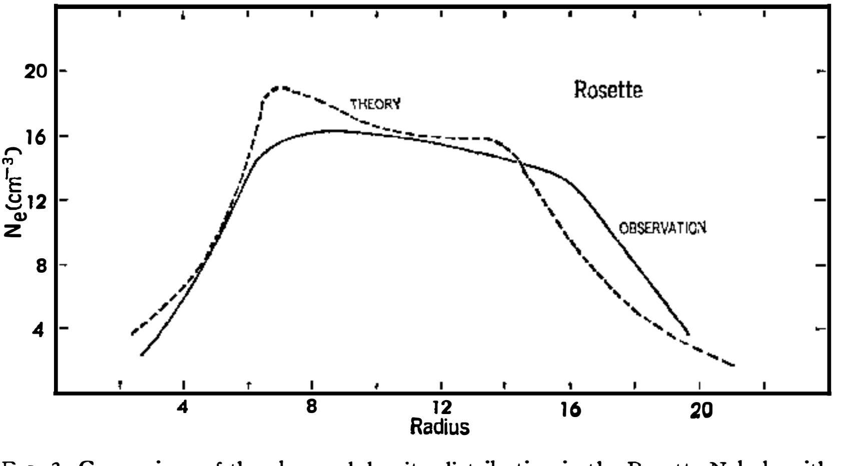

FIG. 3. Comparison of the observed density distribution in the Rosette Nebula with Mathews' (1967) model with an age of 182 000 years.

is seen on satellite ultraviolet photographs (O'Dell, York & Henize 1967). Attributing this ultraviolet brightness to light scattered by particulate material mixed with gas, O'Dell, York & Henize derived an emission distribution for the scattering particles where the number of scatterers per unit volume increases, as the square of the distance from the center of the nebula. The model for the large-scale nebula in Orion is one of density increasing outward to a peak value of about 2.5 atoms/cm^3 at a distance of 60 pc with a rather abrupt diminution beyond that distance. Using stellar model-atmosphere predictions of ionizing flux for the inner stars, these investigators predict an ionization boundary at 42 pc which compares well with the observed value of 46 pc. Interpreting the density minimum as due to radiation pressure acting through the interstellar particles, O'Dell et al. were able to explain the observed structure if the radiation lifetime is about the same as that indicated by the runaway stars, i.e. 3×10^6 years (Blaauw 1964).

The Rosette Nebula.—This object is the best studied and the prototype of the bright nebulae having density decreases towards the center. Figure 3 shows the average of the density profiles derived from two radio investigations (Menon 1962, Bottinelli & Gougenheim 1964). Since these studies only measured the ionized hydrogen, the picture is incomplete, especially since we know that a neutral outer shell does exist. The velocities observed in this nebula have been determined by Fabry-Perot techniques described above. An investigation by Flynn (1965), made at 13 points with an angular resolution of 3 arc min diameter, indicated a velocity dispersion of about 10 km/sec, while a later study by Smith (1967) indicates a much smaller velocity dispersion. It is difficult to discriminate between the two investigations. A cursory examination might indicate a resemblance of the observed density distribution to several of Lasker's (1966a) highly evolved models. However, the quantitative features do not fit very well and this is what prompted the investigations of other forces by Mathews (1967) and Krishna Swamy & O'Dell (1967). We show in Figure 3 the density distribution calculated by Mathews for an initially constant-density nebula that has been evolving for about 3.3×10^5 years. The agreement is quite good and indicates the possible importance of radiation-pressure effects supplementing the ordinary hydrodynamic features. The work of Raimond (1966) finds a large cloud of H I of about $10^5\ M_\odot$ and 50 pc radius. The hydrogen density is about 10 cm^{-3}. The radial velocity (with respect to the local standard of rest) is $+8$ km/sec which agrees, within the probable errors, with the star and H II velocities of $+14$ km/sec. Strong shock compressions have not been observed in the H I zone.

Bright Rims, Instabilities, and Star Formation

Bright rims and globules (of characteristic dimension $\simeq$1 pc) have been described and classified by Pottasch (1956, 1958a, 1958b, 1961) and Osterbrock (1957). These authors have shown that the density of ionized gas in the bright rims is typically larger than the mean density in the nebula by factors of 10 or 100. The radial thickness of the rims increases with spectral type of the exciting star. This, together with intensity profiles and radial velocity measurements (Pottasch 1961), strongly suggests that the bright rims are ionization fronts moving into relatively dense regions of neutral hydrogen ($n \sim 10^4$ or 10^5 cm^{-3}) having masses of $\sim 10^{2\pm1} M_\odot$.

It has been a matter of some interest whether the concentrations observed in the bright rims are produced naturally by some instability inherent in the expanding ionization front or simply represent inhomogeneities existing when the ionizing star formed. The similarity between the bright-rim structures and photographs of the Rayleigh-Taylor instability (Lewis 1950) was pointed out by Spitzer (1954). However, the subsequent observational studies by Pottasch and Osterbrock revealed some morphological differences between the rims and the forms expected from experiment or extensions of the Rayleigh-Taylor instability beyond the linear theory (Frieman 1954, Layzer 1955). Moreover, the precise conditions for Rayleigh-Taylor instability are not present in the bright rims since the acceleration field in the frame of the front may not always be large and a gas flow across the front is always present.

Kahn (1956) showed that a *D*-critical ionization front moving into an isolated neutral cloud can be unstable, provided the ionizing photon flux at the front increases with time. This instability, however, occurs at wavelengths smaller than typical dimensions of bright-rim structures and is essentially damped out when recombinations in the ionized gas are considered. Steady-state plane ionization fronts were first shown to be unstable by Vandervoort (1962) who finds that critical *D* fronts are stable and weak *D* fronts are unstable with normally incident ionizing radiation, and radiation from other directions produces overstable modes. Although the growth rates for the unstable modes found by Vandervoort are generally comparable to the ages of H II regions (4×10^5 years for $\lambda \simeq 1$ pc), Axford (1964b) later showed that these instabilities are damped considerably if recombinations in the H II region near the front are taken into account. In the limit $c_1/c_2 \rightarrow 0$ and for normally incident radiation, Axford finds that weak *D* fronts are unstable only for wavelengths $\lambda \leq 0.2$ pc. Even these instabilities may be inhibited since weak *D* fronts, which are likely to be decelerating, will experience a stabilizing effective gravitational field in the (noninertial) frame of the front. In addition, Saaf (1966) has shown that the growth rates of unstable modes in weak *D* fronts decrease monotonically when the ratio c_1/c_2 increases from zero. Newman & Axford (1967) have recently extended Vandervoort's analysis to strong *D* and weak *R* fronts, including the effects of absorption due to recombinations in the ionized gas. They show that strong *D* fronts are stable, and that weak *R* fronts have unstable modes (for $c_1 = 0$) only if recombinations are included. The instability is mild, however, since the time scale for the growth of unstable modes is never very short compared to

t_{form}, the expected duration of weak R fronts, and these time scales are comparable only for short-wavelength disturbances ($\lambda \leq 6/n_i$ pc).

These results indicate that bright-rim structures are easier to understand in terms of initial inhomogeneities rather than instabilities of the ionization fronts. Of course, the densities in the rims are probably higher than before the surrounding gas became ionized. A number of papers by Dibai (1958, 1960, 1964) and Gershberg (1962) have discussed the interaction of ionization fronts with density inhomogeneities. Dibai & Kaplan (1965) have provided a similarity solution for the spherical isothermal compression of a globule of neutral gas by the surrounding H II medium. Large increases in density and, possibly, star formation can result. Small emission knots have been observed in H II regions (Osterbrock 1967, Velghe 1957), and at least one of these is also a thermal radio source (Wyndham 1966). The recent discovery that radio OH emission is coincident with infrared sources near H II regions (Raimond & Eliasson 1967, Wilson & Barrett 1968, Eliasson & Groth 1968) may also indicate that these are regions of incipient star formation.

Areas of Future Investigation

As shown in the preceding sections of this review, we now have a rather good knowledge of the general features of the evolution of diffuse nebulae; but it is clear that a number of major areas of investigation remain open. We should like to list a few of these problems and possible approaches.

1. The potential for diagnostic study of mass motions within H II regions has only been lightly touched. The application of Fabry-Perot techniques, combining high spatial and wavelength resolution, can provide the necessary information about mass motions. Of particular interest would be the systematic study of several nebulae in lines arising from several different states of ionization, thus probing through different parts of the nebula even at one line-of-sight. The study of the velocities of [O I] would be especially interesting since this line is largely emitted close to the ionization boundary, where significant dynamical changes occur.

2. Radio studies should be continued and refined beyond the present valuable investigations to outline the velocity characteristics in both the H I and H II regions more clearly. The study of the latter, by means of the high-n hydrogen lines, is especially important in those nebulae of high and variable extinction.

3. The newly discovered high surface-brightness (emission measures of 10^6-10^8 cm^{-6} pc but unseen optically) H II regions demand extensive efforts of observation with the best possible spatial and frequency resolution.

4. The infrared nebulae, such as the diffuse source in Orion, need to be studied as to spatial structure and flux distribution across the object.

5. The mechanism of particle destruction within nebulae should be investigated more completely, both observationally and theoretically. More

observations need to be made of the scattered light from diffuse nebulae to see if unambiguous interpretations of the location of the scattering particles can be made. If particles are destroyed at ionization boundaries, one might be able to see the effects by high-dispersion observations of bright rims.

6. Are the globules part of the evolutionary formation of new stars?
7. Why do density inhomogeneities persist in H II regions?

LITERATURE CITED

Abe, Y., Sakashita, S., Ono, Y. 1963, *Progr. Theoret. Phys.*, **30,** 816
Axford, W. I., 1961, *Phil. Trans. Roy. Soc. London A*, **253,** 301
Axford, W. I., 1964a, *Ap. J.*, **139,** 761
Axford, W. I. 1964b, *ibid.*, **140,** 112
Barnard, E. E. 1895, *Pop. Astron.*, **2,** 151
Blaauw, A. 1964, *Ann. Rev. Astron. Ap.*, **2,** 219
Burbidge, G. R., Gould, R. J., Pottasch, S. R. 1963, *Ap. J.*, **138,** 945
Bottinelli, L., Gougenheim, W. 1964, *Ann. Ap.*, **27,** 685
Chandrasekhar, S. 1939, *Stellar Structure*, Chap. 12 (New York: Dover)
Chandrasekhar, S., Wares, G. W., 1949, *Ap. J.*, **109,** 551
Courant, R., Friedrichs, K. O. 1948, *Supersonic Flow and Shock Waves* (New York: Interscience)
Courtes, G. 1960, *Ann. Ap.*, **23,** 115
Courtes, G., Georgelin, Y., Monnet, G., Pourcelot, A. 1968, *Interstellar Ionized Hydrogen*, 571 (Terzian, Y., Ed., New York: W. A. Benjamin)
Dalgarno, A., Rudge, M. R. H. 1964, *Ap J.*, **140,** 800
Davidson, K., Harwit, M. 1967, *Ap. J.*, **148,** 443
Davies, R. D., Tovmassian, H. M. 1963, *MNRAS*, **127,** 45
Dibai, E. A. 1958, *Soviet Astron.*, **2,** 429
Dibai, E. A. 1960, *ibid.*, **4,** 13
Dibai, E. A. 1964, *ibid.*, **7,** 606
Dibai, E. A., Kaplan, S. A. 1965, *Soviet Astron.*, **8,** 520
Dickel, H. 1968, *Ap. J.*, **152,** 651
Eliasson, B., Groth, E. J. 1968, *Ap. J. Letters*, **154,** 217
Flynn, F. H. 1965, *MNRAS*, **130,** 9
Frieman, E. A. 1954, *Ap. J.*, **120,** 18
Gershberg, R. E. 1961, *Izv. Krymsk. Obs.*, **25,** 76
Gershberg, R. E. 1962, *Soviet Astron.*, **5,** 626
Gershberg, R. E., Sheglov, P. V. 1963, *Astron. Zh.*, **41,** 425
Girnstein, H. G., Rohlf, K. 1964, *Z. Ap.*, **59,** 83
Goldberg, L. 1966, *Ap. J.*, **144,** 1225
Goldsworthy, F. A. 1958, *Rev. Mod. Phys.*, **30,** 1062
Goldsworthy, F. A. 1961, *Phil. Trans. Roy. Soc. London A*, **253,** 277
Golesworthy, F. A. 1967, *J. Inst. Math. Appl.*, **3,** 60
Harwit, M. 1962, *Ap. J.*, **136,** 832
Hjellming, R. M. 1966, *Ap. J.*, **143,** 420
Hoglund, B., Mezger, P. G. 1965, *Science*, **150,** 339
Hummer, D. G., Seaton, M. J. 1964, *MNRAS*, **127,** 217
Kahn, F. D. 1954, *Bull. Astron. Soc. Neth.*, **12,** 187
Kahn, F. D. 1956, *IAU Symp. No. 8*, *Rev. Mod. Phys.*, **30,** 1058
Kahn, F. D., Dyson, J. E. 1965, *Ann. Rev. Astron. Ap.*, **3,** 47
Kaler, J. B. 1967, *Ap. J.*, **148,** 925
Kaler, J. B., Aller, L. H., Bowen, I. S. 1965, *Ap. J.*, **141,** 912
Kaplan, S. A. 1959, *Soviet Astron.*, **1,** 183
Kaplan, S. A. 1966, *Interstellar Gas Dynamics* (Oxford: Pergamon)
Krishna Swamy, K. S., O'Dell, C. R. 1967, *Ap. J.*, **157,** 529
Landau, L. D., Lifshitz, E. M. 1958, *Fluid Mechanics* (London: Pergamon)
Langberg, E. 1958, *Phys. Rev.*, **111,** 91
Lasker, B. M. 1966a, *Ap. J.*, **143,** 700
Lasker, B. M. 1966b, *ibid.*, **146,** 5710
Layzer, D. 1955, *Ap. J.*, **122,** 1
Lewis, D. J. 1950, *Proc. Roy. Soc. London A*, **202,** 81
Liller, W., Aller, L. H. 1959, *Ap. J.*, **130,** 45
Mathews, W. G. 1965, *Ap. J.*, **142,** 1120
Mathews, W. G. 1966, *ibid.*, **144,** 206
Mathews, W. G. 1967, *ibid.*, **147,** 965
Mathews, W. G. 1969, *ibid.* (Submitted)
Menon, T. K. 1961, *Publ. Natl. Radio Astron. Obs.*, **1,** 1
Menon, T. K. 1962, *Ap. J.*, **135,** 394
Mezger, P. G., Ellis, S. A. 1968, *Ap. Letters*, **1,** 159
Mezger, P. G., Henderson, A. P. 1967, *Ap. J.*, **147,** 471
Mezger, P. G., Palmer, P. 1968, *Science*, **160,** 29
Mihalas, D. 1964, *Ap. J. Suppl.*, 9, 321
Miller, J. S. 1968, *Ap. J.*, **151,** 473
Morton, D. C. 1967, *Ap. J.*, **147,** 1017
Newman, R. C., Axford, W. E. 1967, *Ap. J.*, **149,** 571
Newman, R. C., Axford, W. E. 1968, *ibid.*, **153,** 595
O'Dell, C. R., Hubbard, W. B. 1965, *Ap. J.*, **142,** 591
O'Dell, C. R., Hubbard, W. B., Peimbert, M. 1966, *Ap. J.*, **143,** 743
O'Dell, C. R., York, D. G., Henize, K. G. 1967, *Ap. J.*, **150,** 835
Oort, J. H. 1954, *Bull. Astron. Inst. Neth.*, **12,** 177
Oort, J. H., Spitzer, L. 1955, *Ap. J.*, **121,** 6

Oster, L. 1961, *Ap. J.*, **134**, 1010
Osterbrock, D. E. 1957, *Ap. J.*, **125**, 622
Osterbrock, D. E. 1967, *Publ. Astron. Soc. Pacific*, **79**, 523
Osterbrock, D. E., Flather, E. 1959, *Ap. J.*, 129, 26
Pack, D. C. 1953, *MNRAS*, **113**, 43
Peimbert, M. 1967, *Ap. J.*, **150**, 825
Pikelner, S. B., Sheglov, P. V. 1968, *Astron. Zh.*, **45**, 953
Pottasch, S. R. 1956, *Bull. Astron. Inst. Neth.*, **13**, 77
Pottasch, S. R. 1958a, *ibid.*, **14**, 29
Pottasch, S. R. 1958b, *IAU Symp. No. 8*, *Rev. Mod. Phys.*, **30**, 1053
Pottasch, S. R. 1961, *The Distribution and Motion of Interstellar Matter in Galaxies*, 205 (Woltjer, W., Ed., New York: Benjamin)
Pottasch, S. R. 1965, *Vistas Astron.*
Raimond, E. 1966, *Bull. Astron. Inst. Neth.*, **18**, 191
Raimond, E., Eliasson, B. 1967, *Ap. J. Letters*, **150**, L171
Richtmyer, R. D., Morton, K. W. 1967, *Difference Methods for Initial Value Problems*, 2nd ed. (New York: Interscience)
Riegel, K. W. 1967, *Ap. J.*, **148**, 87
Rubin, R. H. 1968a, *Ap. J.*, **153**, 761
Rubin, R. H. 1968b, *ibid.*, **154**, 391
Saaf, A. F. 1966, *Ap. J.*, **145**, 116
Savedoff, M. P., Greene, J. 1955, *Ap. J.*, **122**, 477
Schatzman, E., Kahn, F. D. 1955, *IAU Symp. No. 2, Gas Dynamics of Cosmic Clouds*, 163 (Amsterdam: North-Holland)
Seaton, M. J. 1955, *Ann. Ap.*, **18**, 188
Seaton, M. J. 1958, *Rev. Mod. Phys.*, **30**, 979
Sedov, L. I. 1959, *Similarity and Dimensional Methods in Mechanics* (London: Cleaver-Hume Press)
Shain, G., Haze, V. F., Pikelner, S. B. 1954, *Mem. Soc. Roy. Sci. Liège*, *Ser. 4*, **15**, 441
Sheglov, P. V. 1968, *Ap. Letters*, 1, 145
Smith, F. J. 1966, *Planet. Space Sci.*, **14**, 937
Smith, M. 1967, *Proc. IAU*, **13b**, 191
Spitzer, L. 1948, *Ap. J.*, **107**, 6
Spitzer, L. 1949, *ibid.*, **109**, 337
Spitzer, L. 1954, *ibid.*, **120**, 1
Spitzer, L. 1962, *Interstellar Matter in Galaxies*, 98 (Woltjer, W., Ed., New York: W. A. Benjamin)
Spitzer, L. 1968, *Nebulae and Interstellar Matter*, 1 (Middlehurst, B. M., Aller, L. H., Eds., Chicago: Univ. of Chicago Press)
Spitzer, L., Savedoff, M. 1950, *Ap. J.*, **111**, 593
Spitzer, L., Tomasko, H. G. 1968, *Ap. J.*, **152**, 971
Stromgren, B. 1939, *Ap. J.*, **89**, 526
Takayanagi, K., Nishimura, S. 1960, *Publ. Astron. Soc. Japan*, **12**, 77
Taylor, G. I. 1946, *Proc. Roy. Soc. London A*, **186**, 273
Terzian, Y. 1965, *Ap. J.*, **142**, 135
Terzian, Y., Mezger, P. G., Schraml, J. 1968, *Ap. Letters*, **7**, 153
Vandervoort, P. O. 1962, *Ap. J.*, **135**, 212
Vandervoort, P. O. 1963a, *ibid.*, **137**, 381
Vandervoort, P. O. 1963b, *ibid.*, **138**, 426
Vandervoort, P. O. 1964a, *ibid.*, **139**, 869
Vandervoort, P. O. 1964b, *ibid.*, 889
Vandervoort, P. O. 1965a, *ibid.*, **142**, 507
Vandervoort, P. O. 1965b, *ibid.*, 521
Vandervoort, P. O. 1966, *ibid.*, **146**, 104
Vaughn, A. H., Jr. 1967, *Ann. Rev. Astron. Ap.*, **5**, 139
Vaughn, A. H., Jr. 1968, *Ap. J.*, **154**, 87
Velghe, A. G. 1957, *Ap. J.*, **125**, 822
Wade, C. 1958, *Rev. Mod. Phys.*, **30**, 946
Weedman, D. W. 1966, *Ap. J.*, **145**, 965
Wehner, G. K. 1958, *Phys. Rev.*, **112**, 1120
Wilson, O. C., Munch, G., Flather, E., Coffeen, M. 1959, *Ap. J. Suppl.*, **4**, 199
Wilson, W. J., Barrett, A. H. 1968, *Science*, **161**, 778
Würm, K., Perinotto, M. 1965, *Z. Ap.*, **62**, 30
Wyndham, J. D. 1966, *Ap. J.*, **144**, 459

CONTENTS